8th International Conference on Computational and Mathematical Biomedical Engineering - CMBE2024
24–26 June 2024, USA
P. Nithiarasu and R. Löhner (Eds.)

ON THE IMPORTANCE OF MEMBRANE VISCOELASTICITY FOR THE TRANSPORT OF RED BLOOD CELLS IN SHEAR FLOW

Alberto Mantegazza[1,2], Dario De Marinis[2,3], and Marco D. de Tullio[2,3]

[1]Department of Electronics Information and Bioengineering, Politecnico di Milano, 20133 Milano (Italy),
alberto.mantegazza@polimi.it

[2]Department of Mechanics, Mathematics and Management (DMMM), Politecnico di Bari, 70123 Bari (Italy),
{dario.demarinis,marcodonato.detullio}@poliba.it

[3]CNR NANOTEC, Institute of Nanotechnology, 73100 Lecce (Italy)

SUMMARY

Red blood cells (RBCs) are able to deform and flow through the microcirculation thanks to the viscoelastic properties of their membrane. In this study, we present a FSI framework featuring a finite element RBC viscoelastic model coupled with a lattice-Boltzmann method to assess the impact of deformability, internal viscosity, and membrane viscosity on the RBC dynamics in bounded shear flow. We observed that (i) including a viscoelastic membrane influences more the migration timescale than the final equilibrium position along the channel centerline; (ii) the migration timescale is underestimated when the physiological viscosity contrast and the membrane viscosity are neglected.

Key words: *red blood cell, membrane viscosity, lattice Boltzmann method, fluid-structure interaction*

1 INTRODUCTION

In the microcirculation, red blood cells (RBCs) flow through capillaries smaller than their size to deliver oxygen to the surrounding tissues. To meet this physiological need, the RBCs must be able to undergo significant shape changes. The RBC membrane, a soft shell containing the cytoplasm and composed by a lipid bilayer and an inner cytoskeleton, is what ensures that the RBCs can withstand large deformations without being subjected to permanent structural damages. In particular, the lipid bilayer is responsible for the membrane bending rigidity and resistance to area changes, whereas the viscoelastic properties of the cytoskeleton determine the response to shear deformation.
While the membrane elasticity is always taken into consideration in analytical and numerical models, a non-physiological viscosity contrast is often assumed as a simplifying hypothesis despite recent investigations showed that the RBC shape in shear flow is controlled by the cytoplasm viscosity [1]. Additionally, early-on studies revealed a connection between the RBC membrane viscosity and the transient dynamics of deformation [2], but still nowadays the membrane viscosity is typically overlooked in numerical models. Nonetheless, recent numerical studies demonstrated that an accurate RBC model has to account for both the membrane viscosity and viscosity contrast to quantitatively reproduce the membrane relaxation after axial/shear loading of physiological RBCs [3].
In the experimental practice, it is challenging to isolate the contribution of each membrane viscoelastic property to the RBC dynamics. In this context, cell-resolved simulations represent an interesting numerical tool to fully describe the effects of cell viscoelasticity. To this end, we present a fluid-structure interaction (FSI) framework composed of an incompressible lattice-Boltzmann (LB) method [5] to resolve the fluid dynamics inside and outside the RBCs coupled with a finite-element (FE) model to describe the RBC structural dynamics via an immersed-boundary (IB) technique based on the Moving-Least-Square (MLS) approximation [5]. The LBM is supplemented with a tagging procedure to assign a viscosity contrast between the cytoplasm and the plasma, whereas the FE model is complemented with the Standard-Linear-Solid (SLS) model [4] to describe the viscoelastic behavior of the RBC membrane. The aim of this study is to investigate the role of in-plane shear elasticity, viscosity contrast, and membrane viscosity on the RBC transport in bounded shear flow.

2 METHODOLOGY

2.1 FSI strategy: coupling of lattice-Boltzmann method and Finite-Element method

For a generic FSI simulation setup, a 3D Cartesian lattice with fixed nodes is first defined. The computational Eulerian domain Ω is the union of the fluid and interface nodes according to the graphical definition reported in Fig. 1. The fluid continuity and momentum equations are solved in Ω by means of a LB method [5] with a D3Q19 scheme. On the boundary $\partial\Omega$, no-slip, /inlet/outlet boundary conditions are imposed. If an immersed fixed boundary is present, the procedure of Bouzidi is used to impose no-slip conditions at the interface nodes. The evaluation of the forcing term to account for the presence of the viscoelastic RBCs (i.e. the Lagrangian domain Ω_s) is performed using a FE model. An IB technique based on the MLS approximation is adopted to enforce boundary conditions at the fluid-solid interface, thus ensuring the continuity of conserved quantity fields [5].

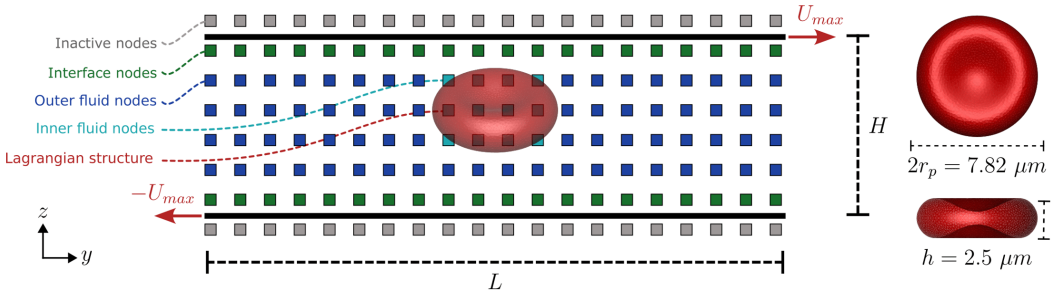

Figure 1: **Graphical representation of the computational domain and simulation setup.** The computational domain is composed by inactive nodes (grey), outer fluid nodes (dark blue), inner fluid nodes (light blue), and interface nodes (green). The union of fluid and interface nodes is the Eulerian domain Ω. The Lagrangian domain Ω_s represents the red blood cell (red). The simulation setup features two infinite parallel plates moving in opposite direction with velocity $(u, v, w) = (0, \pm U_{max}, 0)$ which generates a linear shear rate gradient in the z direction. On the right, the reference configuration of a undeformed red blood cell is shown.

An explicit procedure is used for the time advancement of the FSI solution, as described in the workflow illustrated in Fig. 2. Given the flow field $\boldsymbol{u}(\boldsymbol{x}_k, t)$ on the Eulerian grid, the fluid velocity at the position of a generic Lagrangian node l is interpolated using the MLS technique ($\boldsymbol{U}(\boldsymbol{X}_l, t)$, step I). Next, kinematic boundary conditions are imposed to compute the Lagrangian node velocity ($\dot{\boldsymbol{\mathcal{X}}}(\boldsymbol{X}_l, t)$) and the node position is updated with a 2^{nd}-order scheme (step II-III). Based on the current deformed configuration, the FE model is applied to compute the internal viscoelastic forces due to in-plane membrane elasticity and membrane viscosity using a Skalak strain density energy function and the SLS model, respectively (step IVa-IVb). After adding the force contribution due to out-of-plane bending, volume constraint and repulsion forces (step IVc), a net nodal force $\tilde{\boldsymbol{F}}(\boldsymbol{X}_l, t)$ acting on the Lagrangian node is computed (step V). The net nodal force, evaluated on all Lagrangian nodes, is transferred back to the fluid using the MLS technique ($\hat{\boldsymbol{f}}(\boldsymbol{x}_k, t)$, step VI) to compute the forcing term $\mathcal{F}_i(\boldsymbol{x}, t)$ of the Boltzmann equation (step VII). This forcing term, accounting for the presence of the structure immersed in the fluid, is used to update the probability distribution functions $f_i(\boldsymbol{x}, t)$ representing the fluid particles at position $\boldsymbol{x}$, time t (step VIII). Lastly, the flow field is updated by computing fluid pressure and velocity as first and second moments of $f_i(\boldsymbol{x}, t)$ (step IX).

3 RESULTS AND CONCLUSIONS

3.1 RBC transport in bounded shear flow: computational setup

To investigate the effect of cell viscoelastic properties on the RBC dynamics, we simulated the migration of RBCs subjected to a linear shear flow bounded in the z direction by two parallel walls placed at a distance H (Fig. 1). To generate a linear shear flow, a velocity $v = \pm U_{max}$ is prescribed to the top and bottom wall, respectively. A RBC of radius r_p (confinement ratio $H/r_p = 4$) is placed close to the top wall at $(x_0/W,\ y_0/L,\ z_0/H) = (0.5,\ 0.05,\ 0.8)$. Using U_{max} and r_p as characteristic velocity and length, a particle Reynolds number $Re_p = 1$ is set. No-slip bound-

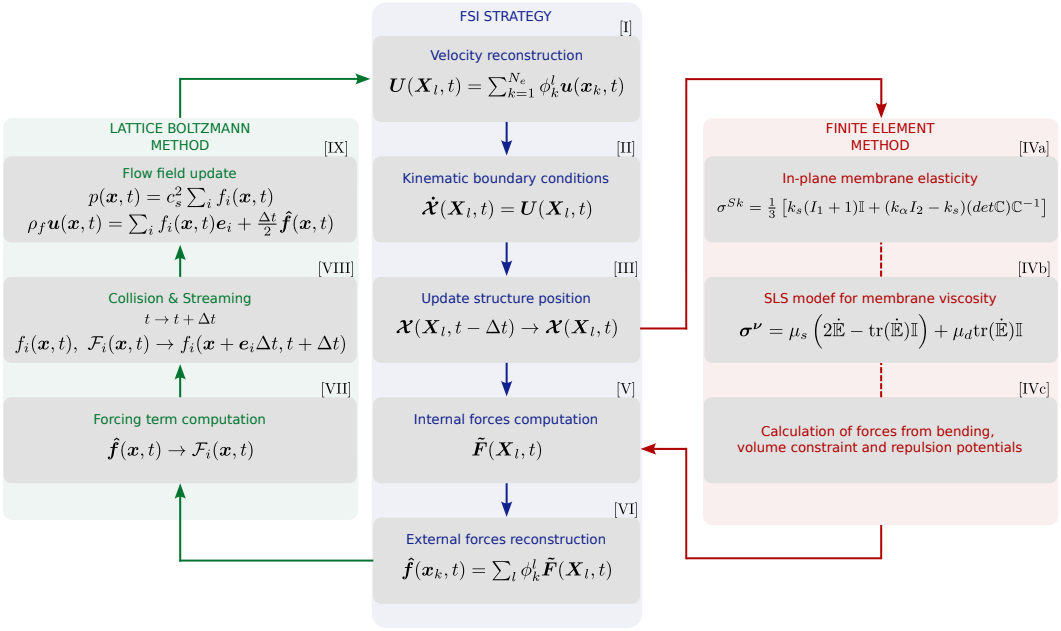

Figure 2: **FSI strategy.** The diagram illustrates the chronological steps of our FSI strategy to couple the fluid dynamics resolved with the LB method and the RBC structural dynamics computed with a FE method.

ary conditions are imposed on the internal surfaces of the walls, cyclic boundary condition are imposed on the inlet/outlet, and periodicity elsewhere. The RBC deformability is controlled by setting the capillary number $Ca = \mu_{out}\dot{\gamma}r_p/k_s$, where k_s is the in-plane shear elastic modulus. The physiological mechanical properties of the RBC are reproduced assigning an elastic shear modulus $k_s = 5 \times 10^{-6}\ N \cdot m^{-1}$, an elastic dilatational modulus $k_\alpha = 50k_s$, and a bending modulus $k_b = 2 \times 10^{-19}\ N \cdot m$. Regarding the SLS model [4], we assume the 2D membrane viscosity to be in the range $\mu_m = 0 \div 3.18 \times 10^{-7}\ m \cdot Pa \cdot s$. Simulations are carried out keeping the membrane viscosity constant $\mu_m = 1.59 \times 10^{-7}\ m \cdot Pa \cdot s$ while investigating the sensitivity to RBC deformability and viscosity contrast ($\widehat{\mu} = \mu_{in}/\mu_{out}$) in the range $Ca = [0.05,\ 0.1,\ 0.2]$, $\widehat{\mu} = [1,\ 5,\ 20]$, respectively. The effect of the viscoelastic properties of the membrane is investigated by performing simulations at $\mu_m = [0,\ 0.64 \times 10^{-7},\ 1.59 \times 10^{-7},\ 3.18 \times 10^{-7}]\ m \cdot Pa \cdot s$ for $Ca = 0.1$ and $\widehat{\mu} = 5$.

3.2 RBC transport in bounded shear flow: effect of RBC viscoelastic properties

In the parameter space that we explored, the RBCs exhibit a periodic solid-like motion until they align in the flow with the major axes lying perpendicularly to the shear plane (Fig. 3a, top contour plot). At steady state, the RBCs keep rolling due to a non-zero velocity field around their membrane (cf. the contour plot of the velocity magnitude at the bottom of Fig. 3a). During the transient flipping motion, the RBCs undergo cyclic phases of compression and stretching. As it could be expected, we observed that the state of deformation is directly proportional to the membrane deformability. Instead, increasing the viscosity contrast or the membrane viscosity had the twofold effect of: (i) introducing a phase lag in the deformation periodicity and reducing the state of deformation; (ii) anticipating the transition from the flipping to the rolling motion.
In terms of RBC migration, we observed that the membrane viscoelasticity and the viscosity contrast affect the migration timescale rather then the final equilibrium position, which was always in the center of the channel (Fig. 3(b)-(d)). Results showed that an impaired deformability, which is often the case for pathological RBCs, leads to a faster migration. Importantly, this finding was visible only if a physiological viscosity contrast is considered ($\widehat{\mu} = 5$, Fig. 3b). We also found that the RBC migration is faster when an idealized viscosity contrast is used ($\widehat{\mu} = 1$, Fig. 3c). Similarly, the migration of a purely elastic RBC is accelerated compared to the case of a RBC featuring a viscoelastic membrane (Fig. 3d). In conclusion, the findings of this study point out that the RBC membrane viscoelasticity has to be considered to accurately model the physiological time-dependent behavior of flowing RBCs.

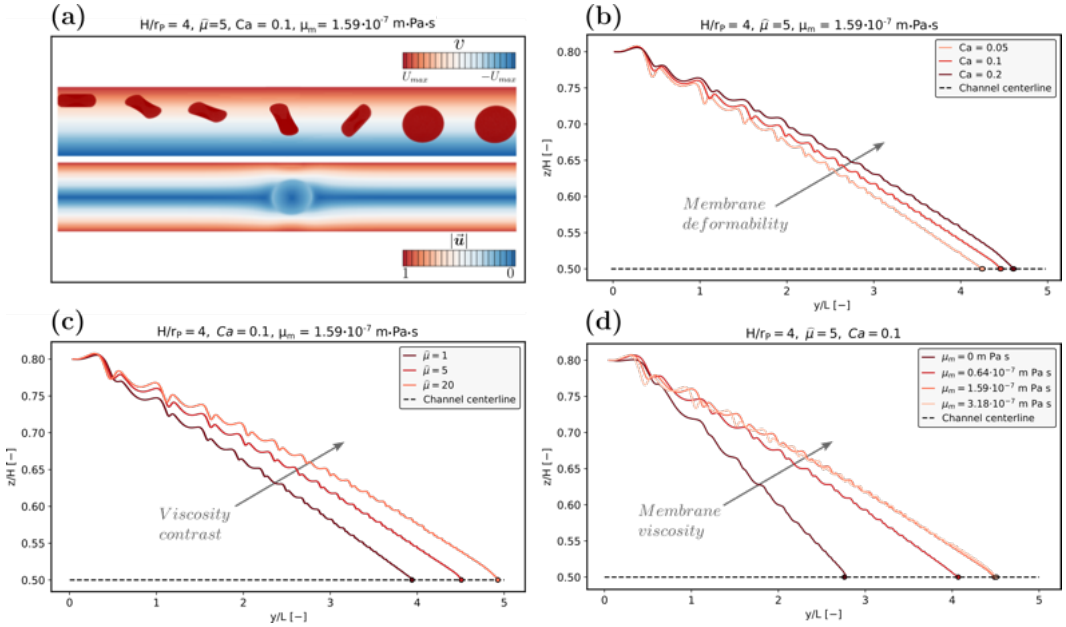

Figure 3: **RBC migration in bounded shear flow.** **(a)** At the top, RBC snapshots taken at progressive time instants are superimposed to the contour plot of the longitudinal velocity v to show the RBC dynamics during the migration. At the bottom, the contour plot of the velocity magnitude ($|\vec{\boldsymbol{u}}|$) at $t/T_{max} = 40\%$ is shown to highlight the non-zero velocity around the RBC after that it has reached the final equilibrium position, which is a sign of rolling motion. The relative RBC longitudinal position (y/L) over time (t/T_{max}) is reported as a function of **(b)** membrane deformability (Ca), **(c)** viscosity contrast ($\widehat{\mu}$), and **(d)** membrane viscosity (μ_m).

DECLARATION OF COMPETING INTEREST

The authors declare that they have no known competing financial interests or personal relationships that could have influenced the results of this study.

ACKNOWLEDGEMENTS

This study was partially supported by BRIEF - Biorobotics Research and Innovation Engineering Facilities, funded by European Union - Next Generation EU, CUP: J13C22000400007. The authors acknowledge the "CNR-NANOTEC Lecce HPC-Cluster - MUR PON Ricerca e Innovazione 2014-2020 - PIR01_00022 Developing nAtional and Regional Infrastructural nodes of dAriaH in iTaly (https://dariah.cnr.it)" for computational resources supporting this work.

REFERENCES

[1] L. Lanotte, S. Mauer, S. Mendez, D. A. Fedosov, J.-M. Fromental, V. Claveria, F. Nicoud, G. Gompper, and M. Abkarian. Red cells' dynamic morphologies govern blood shear thinning under microcirculatory flow conditions. *Proceedings of the National Academy of Sciences of the United States of America*, 113(47):13289-13294, 2016.

[2] R. M. Hochmuth, P. R. Worthy, and E. A. Evans. Red cell extensional recovery and the determination of membrane viscosity. *Biophysical Journal*, 26(1):101–114, 1979.

[3] F. Guglietta, M. Behr, L. Biferale, G. Falcucci, M. Sbragaglia. On the effects of membrane viscosity on transient red blood cell dynamics, *Soft Matter*, 16(26):6191–6205, 2020.

[4] P. Li, and J. Zhang. A finite difference method with subsampling for immersed boundary simulations of the capsule dynamics with viscoelastic membranes. *International Journal for Numerical Methods in Biomedical Engineering*, 35(6):e3200, 2019.

[5] D. De Marinis, A. Mantegazza, A. Coclite, and M. D. de Tullio. A fluid-structure interaction method for soft particle transport in curved microchannels. *Computer Methods in Applied Mechanics and Engineering*, 418:116592, 2024.